

Probing Intergalactic Magnetic Fields with Gamma Rays from Blazars

Susumu Inoue*

Institute for Cosmic Ray Research, University of Tokyo, Kashiwa, Japan

E-mail: sinoue@icrr.u-tokyo.ac.jp

Keitaro Takahashi

Graduate School of Science and Technology, Kumamoto University, Kumamoto, Japan

E-mail: keitaro@sci.kumamoto-u.ac.jp

Masaki Mori

Department of Physical Sciences, Ritsumeikan University, Kusatsu, Japan

E-mail: morim@fc.ritsumei.ac.jp

Kiyotomo Ichiki

Department of Physics and Astrophysics, Nagoya University, Nagoya, Japan

E-mail: ichiki@a.phys.nagoya-u.ac.jp

High-energy gamma rays from blazars may be accompanied by secondary emission components due to e^-e^+ pairs produced in interactions of primary TeV photons with the extragalactic background light, which can provide a unique probe of weak intergalactic magnetic fields (IGMFs) through their characteristic time delay (pair echos) or angular extension (beamed pair halos). Together with theoretical expectations, we briefly review recent claims of lower bounds to IGMF strengths in the range $B \sim 10^{-18} - 10^{-15}$ G inferred from observational upper limits on such components, and caution that they are dependent on unproven assumptions regarding the primary emission during epochs unobserved by TeV telescopes. Utilizing only simultaneously observed GeV-TeV light curves with a minimum of such assumptions, our conservative limits on the pair echo emission for Mrk 501 imply a weak bound of $B \gtrsim 10^{-20}$ G for a field coherence length of 1 kpc, which is nevertheless evidence for non-zero IGMFs that is more robust compared to previous studies. We comment on future prospects in the CTA era, emphasizing the need to positively detect the secondary components in order to obtain more definitive information on IGMFs.

AGN Physics in the CTA Era - AGN2011,

May 16-17, 2011

Toulouse, France

*Speaker.

1. Introduction

Although their existence is yet to be unambiguously confirmed, the possibility that weak but ubiquitous magnetic fields were generated in the early Universe has attracted considerable attention [1, 2]. Such “cosmological” magnetic fields are potentially important from at least two perspectives. First, by serving as the seed fields for subsequent amplification by galactic dynamo mechanisms, they could have been the ultimate origin of the magnetic fields seen today in galaxies and clusters of galaxies [2, 3]. Second, in some regions such as the centers of intergalactic voids, they may have survived to the present day as intergalactic magnetic fields (IGMFs) without being affected by later magnetization from astrophysical sources [4, 5, 6], and therefore may provide us with valuable, fossil information about physical processes in the early Universe. So far, various mechanisms have been proposed for the generation of such cosmological magnetic fields, including different types of cosmological phase transitions [7, 8, 9] or processes related to early galaxy formation and cosmic reionization [10, 11, 12], with predicted field amplitudes in the range $B \sim 10^{-25} - 10^{-15}$ G. While they may suffice as seeds for galactic dynamos, such tiny magnetic fields are extremely difficult to confirm observationally through conventional methods such as Faraday rotation measurements [13] or their effect on cosmic microwave background anisotropies [14].

A potentially powerful probe of such weak IGMFs may be offered by secondary GeV-TeV components accompanying extragalactic TeV sources such as blazars or gamma-ray bursts (GRBs), resulting from inverse Compton (IC) emission by e^-e^+ pairs produced via intergalactic $\gamma\gamma$ interactions among primary TeV photons and infrared-UV photons of the extragalactic background light (EBL). Such emission components may be observable either as “pair echos” that arrive with a time delay relative to the primary emission [15, 16, 17, 18, 19, 20, 21], or as “beamed pair halos”¹ with a spatial extension around the primary source [23, 24, 25, 26], which depend on the properties of the intervening IGMFs while being insensitive to galactic-scale magnetic fields either local to the source or the observer.

Although there have been no clear observational indications for either pair echo or halo emission so far (c.f. [27, 28]), a number of recent studies have claimed to derive lower bounds to IGMF strengths in the range $B \sim 10^{-18} - 10^{-15}$ G from upper limits to such components obtained by GeV-TeV observations of selected blazars [29, 30, 31, 32, 33, 34, 35]. First we provide a short critique of these studies and warn that they are all contingent to varying degrees on questionable or unjustified assumptions concerning the primary emission during periods not covered by TeV telescopes. Our own analysis [36] is then presented for the pair echo emission in the blazar Mrk 501 that is nearly free of such assumptions, utilizing only simultaneous GeV-TeV light curves observed by VERITAS, MAGIC and *Fermi*-LAT during a multiwavelength campaign in 2009 that included a TeV flare [37]. We arrive at a conservative bound of $B \gtrsim 10^{-20}$ G at 90% confidence level for a field coherence length of 1 kpc, which is weaker compared to previous studies but nevertheless more robust evidence for a non-zero IGMF. We end with brief remarks on future prospects, empha-

¹Note that “pair halos” as originally discussed by [22] focused on the case where IGMFs are strong enough to entirely isotropize the pairs and the consequent secondary emission, in which case its properties do not depend explicitly on the IGMF. In order to differentiate from such isotropic pair halos, here we use the term “beamed pair halos” to refer to secondary emission from pairs that are only mildly deflected in weaker IGMFs.

sizing the potential of the Cherekov Telescope Array (CTA) for gaining more definitive information on IGMFs through positive detections of the pair echo or halo emission.

2. Basics of pair echos and beamed pair halos

First we briefly go over some basic aspects of pair echo and beamed pair halo emission, choosing fiducial numbers relevant for Mrk 501. For more details, we refer the reader to Ichiki et al. [18] and Neronov & Semikoz [24] on the physics of pair echos and halos in general, and to Takahashi et al. [36] on the specific application to Mrk 501.

Primary gamma-rays with energy $E_\gamma \gtrsim 1$ TeV emitted from an extragalactic source at relatively low redshift ($z \ll 1$) have mean free path $\lambda_{\gamma\gamma} = 1/(0.26\sigma_T n_{\text{IR}}) = 190 \text{ Mpc } (n_{\text{IR}}/0.01 \text{ cm}^{-3})^{-1}$ for $\gamma\gamma$ pair production interactions with the EBL in the infrared (IR) band, where σ_T is the Thomson cross section and n_{IR} is the number density of IR EBL photons most relevant for the interactions. The produced pairs with energy $E_e \approx E_\gamma/2$ give rise to the secondary emission by IC upscattering of ambient cosmic microwave background (CMB) photons to average energy $\langle E_{\text{sec}} \rangle = 2.7T_{\text{CMB}}\gamma_e^2 = 2.5 \text{ GeV } (E_\gamma/2 \text{ TeV})^2$, where $\gamma_e = E_e/m_e c^2$ is the Lorentz factor of the pairs and $T_{\text{CMB}} = 2.7 \text{ K}$ is the CMB temperature. Thus, primary gamma-rays in the range $E_\gamma \simeq 1 - 5$ TeV induce secondary photons with typical energies $E_{\text{sec}} \simeq 1 - 10$ GeV. The IC mean free path of the pairs is $\lambda_{\text{IC,scat}} = 1/(\sigma_T n_{\text{CMB}}) = 1.2 \text{ kpc}$, where $n_{\text{CMB}} \approx 420 \text{ cm}^{-3}$ is the CMB photon number density. The pairs upscatter CMB photons successively until they lose most of their energy after propagating an IC cooling length $\lambda_{\text{IC,cool}} = 3m_e^2/(4E_e\sigma_T U_{\text{CMB}}) = 350 \text{ kpc } (E_e/1 \text{ TeV})^{-1}$, where U_{CMB} is the CMB energy density. The length scales for $\lambda_{\gamma\gamma}$ and $\lambda_{\text{IC,cool}}$ imply that the secondary pairs typically arise in locations far removed from the source on scales of intergalactic voids, whereas the pairs propagate only for short distances within such regions while generating the secondary emission.

The secondary emission arrives at the observer with a time delay relative to the primary emission, caused by the effects of angular spreading in pair production and IC interactions, as well as by deflections of the pairs in intervening magnetic fields. The typical delay time due to angular spreading is [18]

$$\Delta t_{\text{ang}} = \frac{1}{2\gamma_e^2}(\lambda_{\gamma\gamma} + \lambda_{\text{IC,cool}}) \approx 3 \times 10^3 \text{ sec} \left(\frac{E_{\text{sec}}}{1 \text{ GeV}} \right)^{-1} \left(\frac{n_{\text{IR}}}{0.01 \text{ cm}^{-3}} \right)^{-1}. \quad (2.1)$$

That due to magnetic deflections is

$$\Delta t_{\text{B}} = \frac{1}{2}(\lambda_{\gamma\gamma} + \lambda_{\text{IC,cool}})\langle \theta_{\text{B}}^2 \rangle, \quad (2.2)$$

where

$$\langle \theta_{\text{B}}^2 \rangle^{1/2} = \begin{cases} \frac{\lambda_{\text{IC,cool}}}{r_{\text{L}}}, & \lambda_{\text{coh}} \gg \lambda_{\text{IC,cool}} \\ \left(\frac{\lambda_{\text{IC,cool}} \lambda_{\text{coh}}}{6} \right)^{1/2} \frac{1}{r_{\text{L}}}, & \lambda_{\text{coh}} \ll \lambda_{\text{IC,cool}} \end{cases} \quad (2.3)$$

is the variance of the magnetic deflection angle in terms of the gyroradius $r_{\text{L}} = E_e/eB$ and field coherence length λ_{coh} , and the two cases correspond to whether the fields can be considered uniform

or randomly tangled over the length scale of pair propagation. In the latter case,

$$\Delta t_B \approx 2 \times 10^4 \text{ sec} \left(\frac{E_{\text{sec}}}{1 \text{ GeV}} \right)^{-3/2} \left(\frac{B}{10^{-19} \text{ G}} \right)^2 \left(\frac{\lambda_{\text{coh}}}{1 \text{ kpc}} \right) \left(\frac{n_{\text{IR}}}{0.01 \text{ cm}^{-3}} \right)^{-1}. \quad (2.4)$$

Hereafter we fiducially take $\lambda_{\text{coh}} = 1 \text{ kpc}$ as expected in some models of IGMF generation [11], but the results are scalable to other values of λ_{coh} since it enters only through the combination $B^2 \lambda_{\text{coh}}$ and only when $\lambda_{\text{coh}} \lesssim \lambda_{\text{IC,cool}}$. The total delay time is approximately $\Delta t = \Delta t_{\text{ang}} + \Delta t_B$, and the magnetic field properties are reflected in the delay as long as $\Delta t_{\text{ang}} \lesssim \Delta t_B$.

In order to evaluate the spectra and light curves of the pair echo emission that arrive with such time delays, one first calculates the flux of secondary pairs based on a given light curve of the primary emission and the energy-dependent $\gamma\gamma$ optical depth from a model for the EBL, and then obtains a time-dependent echo spectrum by properly incorporating the geometrical effects of photon propagation paths on the delay, the detailed procedure of which is described in [18]. Note that the pair echo fluence is determined by the total amount of absorbed primary gamma rays and thus independent of the IGMF properties, in contrast to the pair echo flux which is roughly given by the fluence divided by Δt . Weaker IGMFs generally give higher echo fluxes, as long as the time delay does not become dominated by angular spreading and the echo flux remains sensitive to B . For $\lambda_{\text{coh}} = 1 \text{ kpc}$, Δt_B approaches Δt_{ang} if $B \sim 10^{-20} \text{ G}$. The formulation of Ichiki et al. [18] was employed in Murase et al. [19] before the launch of *Fermi* to demonstrate that detection or even upper limits on the pair echo emission induced by TeV flares of blazars such as Mrk 501 or PKS 2155-304 can effectively constrain IGMFs around $B \sim 10^{-21} - 10^{-19} \text{ G}$.

If IGMF strengths turn out to be in a stronger range of $B \sim 10^{-16} - 10^{-12} \text{ G}$, the magnetic deflections may become large enough for the angular extension of the secondary emission to be resolvable by gamma-ray telescopes as beamed pair halos [23, 24]. The typical angular extension for a source at $z \ll 1$ is

$$\Theta_B = \langle \theta_B^2 \rangle^{1/2} \frac{\lambda_{\gamma\gamma}}{D} \approx 0.26^\circ \left(\frac{E_{\text{sec}}}{1 \text{ GeV}} \right)^{-3/4} \left(\frac{B}{10^{-14} \text{ G}} \right) \left(\frac{\lambda_{\text{coh}}}{1 \text{ kpc}} \right)^{1/2} \left(\frac{D}{130 \text{ Mpc}} \right)^{-1} \left(\frac{n_{\text{IR}}}{0.01 \text{ cm}^{-3}} \right)^{-1}, \quad (2.5)$$

where D is the distance to the source, and the numerical expression corresponds to the case when $\lambda_{\text{coh}} \ll \lambda_{\text{IC,cool}}$. The angular profile of the halo emission can be evaluated by accounting for the propagation geometry in a way analogous to the pair echo calculation, as long as one knows the spectrum and relevant time history of the primary emission.

Note that if IGMFs are even stronger, $B \gtrsim 10^{-12} \text{ G}$, the pairs can be completely isotropized before emitting secondary photons, and the resultant pair halo will no longer depend explicitly on the IGMF properties [22]. Detection of such isotropic pair halos will nevertheless be meaningful, since it will provide not only indicative lower bounds on the IGMF, but also important information regarding the multi-TeV spectrum and beaming angle of the primary emission, as well as a unique probe of the EBL.

3. Observational bounds on intergalactic magnetic fields

3.1 Previous studies

By studying the spectra of selected TeV blazars for which *Fermi* observations only gave upper limits, Neronov & Vovk [29] first claimed a lower bound on the IGMF of $B \gtrsim 3 \times 10^{-15}$ G, arguing that if the IGMF was weaker, the resulting secondary component would exceed the GeV limits. This was followed by other studies that also gave similar results [31, 32, 33].

However, one must beware that such IGMFs entail extremely long time delays, $\Delta t_B \approx 7 \times 10^5 \text{ yr} (E_{\text{echo}}/1 \text{ GeV})^{-3/2} (B/3 \times 10^{-15} \text{ G})^2 (r_{\text{coh}}/1 \text{ kpc}) (n_{\text{IR}}/0.01 \text{ cm}^{-3})^{-1}$. Thus, as pointed out by Dermer et al. [34], an implicit but crucial assumption in deriving these bounds was that the TeV emission has been persistent for at least the past 10^6 years, at the level observed in these objects on a small number of specific dates in the last several years. This assumption is quite questionable, because TeV blazars are generally known to be highly variable. Indeed, for sufficiently well observed objects such as Mrk 421 ([38, 39] and references therein), the TeV flux is known to fluctuate by as much as two orders of magnitude over timescales of several years and less, as is clear in Fig.1. Thus it is not obvious at all whether the TeV flux and spectra adopted in the above studies to evaluate the secondary emission represent an average level for the source over Myr timescales, or is instead considerably higher or lower.

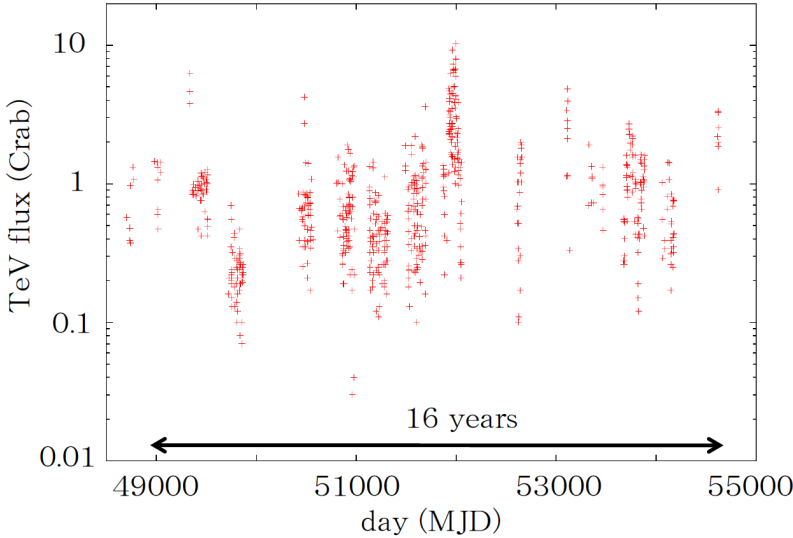


Figure 1: TeV light curve of Mrk 421 over a time span of 16 years, obtained from the DESY unified format gamma-ray data website (<http://www-zeuthen.desy.de/multi-messenger/GammaRayData/index.html>).

Bounds of order $B \gtrsim 10^{-15}$ G were also derived by Aleksic et al. [30] from the non-detection of beamed pair halos around Mrk 421 and Mrk 501 by the MAGIC telescope. However, this again implies very long time delays $\Delta t_B \sim 10^5$ yr. In order to obtain reliable IGMF bounds by comparing the data with expectations for the surface brightness of the halo, one must have knowledge of the entire history of the primary TeV emission over such timescales. This is certainly not yet available from direct observations, so unless the halo component is actually detected, studies based

on only upper limits must resort to unproven assumptions on the past TeV activity on timescales approaching the lifetimes expected for radio-loud AGNs [40].

With a more relaxed assumption that TeV gamma-rays from the blazar 1ES 0229+200 was steady only during the years 2005 to 2009 when Cherenkov telescope observations took place, Dermer et al. [34] derived a much weaker lower bound of order $B \gtrsim 10^{-18}$ G. However, even this assumption is not entirely satisfactory, since the time coverage of TeV observations actually conducted during this period was very sparse, being only several days in 2005, 2006 and 2009. Taylor et al. [35] have presented similar analyses for a few blazars with analogous assumptions on their TeV activity during unobserved periods over timescales of a few years, obtaining comparable bounds.

3.2 Our analysis for Mrk 501

In view of the shortcomings of previous studies, we aim to constrain the pair echo component from Mrk 501 and derive lower bounds on the IGMF relying solely on observed data from a multiwavelength campaign over a few months in 2009 [37]. We make use of the basic formulation of Ichiki et al. [18] outlined above, but with additional improvements in order to accommodate the finite probability of pair production near the observer, which must be considered for Mrk 501 whose $D \sim 130$ Mpc can be comparable to $\lambda_{\gamma\gamma}$ [36]. We clarify what we employ for the primary TeV spectra and light curves. A TeV flare was observed for at least three days from MJD 54953; however, it may have continued for a longer time, or even separate flares could have occurred over the following weeks, as can be speculated from the hard, concurrent 30-day *Fermi*-LAT spectrum [37]. Nevertheless, we choose to be conservative and assume that there is no other flare state during the campaign besides the three days seen by VERITAS. Although the quiescent state was also only sparsely sampled at TeV, since both VERITAS and MAGIC measured a consistent flux and spectrum at separate times, we postulate that the quiescent emission is steady over the period covered by the TeV telescopes, the sole assumption we make regarding TeV activity not directly observed. Thus, we consider the primary light curve to consist of a flare state with a top-hat shape for the 3 days MJD 54953-54955, together with a steady quiescent state for the preceding 46 days MJD 54907-54952 as well as the ensuing 49 days MJD 54956-55004. The primary flux and spectrum for each state are chosen such that they are compatible with those observed by VERITAS after accounting for intergalactic $\gamma\gamma$ absorption with the EBL model of Franceschini et al. [41], and are described by the power-law functional form $\log F(E) = \log K - a \log(E/\text{TeV})$ with $K = 9 \times 10^{-11}$ ph/cm²/sec/TeV and $a = 2.0$ for the flare state, and $K = 2 \times 10^{-11}$ ph/cm²/sec/TeV and $a = 2.3$ for the quiescent state. Minimum and maximum cutoffs are also imposed at 0.1 TeV and 5 TeV, respectively, the latter corresponding to the highest energy photons detected by VERITAS and MAGIC. Comparing the pair echo emission calculated in this way with the observed GeV limits gives conservative lower bounds on the IGMF, since any additional primary emission, outside either the above time interval or the above spectral range, would only add to the pair echo flux and lead to tighter bounds.

Our results are as follows. Fig. 2 shows the spectra of the primary and pair echo emission for the flare and quiescent states when $B = 10^{-20}$ G and $\lambda_{\text{coh}} = 1$ kpc. The primary spectra are displayed both with and without intergalactic $\gamma\gamma$ absorption, the latter to be compared with the absorption-corrected VERITAS data [37]. The echo from the flare state is plotted at observer times

$t = 1, 10$ and 100 days after the flare, fading progressively on timescales approximately corresponding to Δt . In contrast, here the echo due to the quiescent state is essentially stationary on the timescale of the campaign and independent of B . Note, however, that for stronger B with accordingly longer Δt_B , even this echo component can be nonstationary, particularly at low energies, since the “quiescent state” as defined above only lasts for ~ 100 days. Only when the primary emission persists at a steady level for a time considerably longer than Δt_B does the echo reach a stationary condition [34].

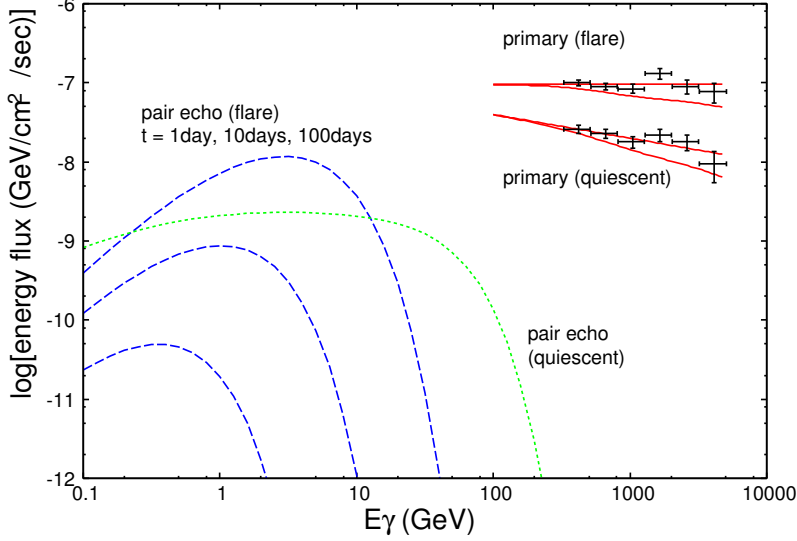


Figure 2: Spectra of the primary and pair echo emission of Mrk 501 for the case $B = 10^{-20}$ G. The primary spectra for the flare and quiescent states are each shown with (long-dashed) and without (solid) intergalactic $\gamma\gamma$ absorption, along with the absorption-corrected data from VERITAS observations. Also plotted are the echo from the flare state at observer time $t = 1, 10$ and 100 days after the flare (dashed, from top to bottom), as well as the echo from the quiescent state (dotted).

The light curves of the pair echo in the 1-10 GeV band after the onset of the TeV flare on MJD 54953 are plotted in Fig. 3 for different values of B . The flux initially rises over the duration of the primary flare, and then decays roughly exponentially on timescales of order Δt as the primary emission switches to the quiescent state. At sufficiently late times, only the quiescent emission contributes to the echo and its flux approaches a steady level. For weaker B , the echo flux responds to changes of the primary flux more quickly by virtue of the shorter Δt_B , and the peak flux is larger and more susceptible to observational limits.

Thus, in order to observationally constrain IGMFs around $B \sim 10^{-20} - 10^{-19}$ G, GeV-band light curves with time resolution of order a day are necessary. We analyzed the *Fermi*-LAT data to obtain 1-10 GeV gamma-ray fluxes and upper limits with 1-day time binning. Since the photon statistics is small, we adopted the aperture photometry method, i.e., events falling within one degree from the source were counted. Background events are essentially negligible above 1 GeV in one-day bins at the high Galactic latitude of Mrk 501. The results are compared with the pair echo expectations in Fig. 3. Most are upper limits, which is not surprising given the limited sensitivity of *Fermi*-LAT with such short integration times. The strongest limits come from the second, third and fourth days, being comparable to the pair echo predictions for $B \lesssim 10^{-20}$ G and providing important

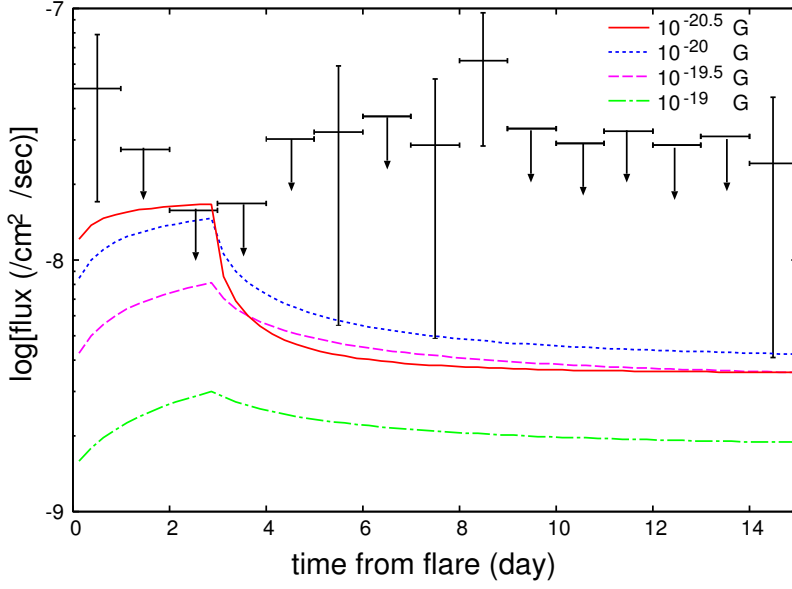


Figure 3: Light curve of Mrk 501 in the 1-10 GeV band from the onset of the TeV flare on MJD 54953. Pair echo expectations for $B = 10^{-20.5}, 10^{-20}, 10^{-19.5}, 10^{-19}$ G (curves from top to bottom) are compared with *Fermi*-LAT data binned at 1-day intervals using the aperture photometry method, where errors (vertical bars) or upper limits (downward arrows) are at 68% confidence level.

lower bounds on IGMFs of this order, while higher values of B cannot be usefully constrained by the current analysis. Note that primary emission in the GeV range is also generally expected and should contribute significantly to the LAT light curve, which implies that the actual pair echo flux is even lower and the true IGMF lower bounds stronger. However, given the lack of reliable knowledge on the primary GeV spectra and variability, we restrict ourselves to conservative constraints by not accounting for any such components (c.f. [34, 35]).

Through a quantitative examination of the probability of consistency between the daily flux upper limits from *Fermi*-LAT and pair echo predictions for different values of B , we arrive at our main result that $B \gtrsim 10^{-20}$ G at about 90% confidence level, determined mostly by the limits from the second through fourth days. We have also carried out similar analyses for other energy bands < 1 GeV or > 10 GeV but were not able to derive significant constraints, as can be expected from Fig. 2.

In summary, by comparing the daily GeV flux upper limits from *Fermi*-LAT for the blazar Mrk 501 during and after its TeV flare in 2009 with the expected light curves for the associated pair echo emission, we have derived lower bounds on IGMF strengths of $B \gtrsim 10^{-20}$ G at 90% confidence level for a field coherence length $\lambda_{\text{coh}} = 1$ kpc. This result can be roughly scaled for other values of λ_{coh} as

$$B \gtrsim 5 \times 10^{-22} \text{ G} \max \left[\left(\frac{\lambda_{\text{coh}}}{350 \text{ kpc}} \right)^{-1/2}, 1 \right]. \quad (3.1)$$

This bound is considerably weaker compared to other recent results obtained through similar methods, which, however, all relied on unproven assumptions regarding the TeV emission during unobserved periods on timescales of years [34, 35] or much longer [29, 30, 31, 32, 33]. In contrast,

our analysis is entirely free of such assumptions other than for the quiescent state, and thus can be considered the most robust indication so far for the existence of non-zero IGMFs.

4. Prospects in the CTA era

Future observational progress can be expected in different directions. First, regular, long-term coverage of the multi-TeV emission of blazars by wide-field facilities such as HAWC² or LHAASO should greatly improve our knowledge of their TeV activity on timescales of years to decades, giving us a much better handle on the light curve of the primary emission as input for more reliable predictions of the pair echo properties. Second, detailed measurements of spectral variability with higher sensitivity and time resolution over a wider energy band should become available with CTA³, potentially allowing us to disentangle and positively identify the echo component from the primary emission, and thereby probing very weak IGMFs in the range $B \sim 10^{-20} - 10^{-16}$ G that may otherwise be impossible. Third, if IGMFs are stronger, $B \sim 10^{-16} - 10^{-12}$ G, the spatially-extended, beamed pair halo emission may be detectable and resolvable by CTA by virtue of its high angular resolution, in which case one would probe not only IGMFs but also the lifetime of TeV activity for the source [42]. On the theoretical side, some important issues concerning the propagation of pairs in weak IGMFs warrant further investigation [43]. Such advances will surely open a new window onto the study of cosmic magnetic fields as well as provide new insight into the global activity of blazar AGNs.

Acknowledgments

This work is supported by Grants-in-Aid from the Ministry of Education, Culture, Sports, Science and Technology (MEXT) of Japan, No. 22540278 (SI), No. 21840028 (KT), No. 22540315 (MM), No. 21740177, No. 22012004 (KI) and for the global COE program “The Next Generation of Physics, Spun from Universality and Emergence” at Kyoto University and “Quest for Fundamental Principles in the Universe: from Particles to the Solar System and the Cosmos” at Nagoya University.

References

- [1] D. Grasso & H. R. Rubinstein, *Phys. Rep.* **348** (2001) 163
- [2] L. M. Widrow, *Rev. Mod. Phys.* **74** (2002) 775
- [3] R. M. Kulsrud & E. G. Zweibel, *Rep. Prog. Phys.* **71** (2008) 0046091.
- [4] S. R. Furlanetto & A. Loeb, *ApJ* **556** (2001) 619.
- [5] P. P. Kronberg, Q. W. Dufton, H. Li & S. A. Colgate, *ApJ* **560** (2001) 178.
- [6] S. Bertone, C. Vogt & T. Enßlin, *MNRAS* **370** (2006) 319.
- [7] M. S. Turner & L. M. Widrow, *Phys. Rev. D* **37** (1988) 2743.

²<http://hawc.umd.edu/>

³<http://www.cta-observatory.org/>

- [8] G. Sigl, A. V. Olinto & K. Jedamzik, *Phys. Rev. D* **55** (1997) 4582.
- [9] K. Ichiki, K. Takahashi, H. Ohno, H. Hanayama & N. Sugiyama, *Sci* **311** (2006) 827.
- [10] N. Y. Gnedin, A. Ferrara & E. G. Zweibel, *ApJ* **539** (2000) 505.
- [11] M. Langer, N. Aghanim & J.-L. Puget, *A&A* **443** (2005) 367.
- [12] F. Miniati & A. R. Bell *ApJ* **729** (2011) 73.
- [13] P. P. Kronberg, *Rep. Prog. Phys* **57** (1994) 325.
- [14] J. D. Barrow, P. G. Ferreira & J. Silk, *Phys. Rev. Lett.* **78** (1997) 3610.
- [15] R. Plaga, *Nat* **374** (1995) 430.
- [16] Z. G. Dai, B. Zhang, L. J. Gou, P. Mészáros & E. Waxman, *ApJ* **580** (2002) L7.
- [17] S. Razzaque, P. Mészáros & B. Zhang, *ApJ* 613 (2004) 1072.
- [18] K. Ichiki, S. Inoue, & K. Takahashi, *ApJ* **682** (2008) 127.
- [19] K. Murase, K. Takahashi, S. Inoue, K. Ichiki & S. Nagataki, *ApJ* **686** (2008) L67.
- [20] K. Takahashi, K. Murase, K. Ichiki, S. Inoue & S. Nagataki, *ApJ* **687** (2008) L5.
- [21] K. Takahashi, S. Inoue, K. Ichiki & T. Nakamura, *MNRAS* **410** (2011) 2741.
- [22] F. A. Aharonian, P. S. Coppi & H. J. Völk, *ApJ* bf 423 (1994) L5.
- [23] A. Neronov & D. V. Semikoz, *JETP Lett.* **85** (2007) 473.
- [24] A. Neronov & D. V. Semikoz, *Phys. Rev. D* **80** (2009) 123012.
- [25] A. Elyiv, A. Neronov, & D. V. Semikoz, *Phys. Rev. D* **80** (2009) 023010.
- [26] K. Dolag, M. Kachelrieß, S. Ostapchenko & R. Tomás, *ApJ* **703** (2009) 1078.
- [27] S. Ando & A. Kusenko, *ApJ* **722** (2010) L39.
- [28] A. Neronov, D. V. Semikoz, P. G. Tinyakov & I. I. Tkachev, *A&A* **526** (2011) A90.
- [29] A. Neronov & I. Vovk, *Sci* **328** (2010) 73.
- [30] J. Aleksic et al., *A&A* **524** (2010) A77.
- [31] F. Tavecchio, G. Ghisellini, L. Foschini, G. Bonnoli, G. Ghirlanda & P. Coppi, *MNRAS* **406** (2010) L70.
- [32] F. Tavecchio, G. Ghisellini, G. Bonnoli & L. Foschini, *MNRAS* **414** (2011) 3566.
- [33] K. Dolag, M. Kachelrieß, S. Ostapchenko & R. Tomás, *ApJ* **727** (2011) L4.
- [34] C. D. Dermer, M. Cavadini, S. Razzaque, J. D. Finke & B. Lott, *ApJ* **733** (2011) L21.
- [35] A. M. Taylor, I. Vovk & A. Neronov, *A&A* **529** (2011) A144.
- [36] K. Takahashi, M. Mori, K. Ichiki & S. Inoue, *ApJL*, in press [arXiv:1103.3835].
- [37] A. A. Abdo et al., *ApJ* **727** (2011) 129.
- [38] V. A. Acciari et al. 2011, *ApJ* **738** (2011) 25.
- [39] B. Bartoli et al., *ApJ* bf 734 (2011) 110.
- [40] P. Parma, M. Murgia, H. R. de Ruiter & R. Fanti, *New. Astron. Rev.* **46** (2002) 313.
- [41] A. Franceschini, G. Rodighiero & M. Vaccari, *A&A* **487** 837.
- [42] A. Neronov, D. Semikoz, M. Kachelrieß, S. Ostapchenko & A. Elyiv, *ApJ* **719** (2010) L130.
- [43] A. E. Broderick, P. Chang & C. Pfrommer, *ApJ* submitted [arXiv:1106.5494].